Actuator Disc Simulations of Influence of Wind Shear on Power Production of Wind Turbines

Niels Troldborg*, Mac Gaunaa* and Robert Mikkelsen†
*Wind Energy Department, Risø, National Laboratory, DTU, DK-4000 Roskilde, Denmark
†Department of Mechanical Engineering, Fluid Mechanics Section, Technical University of Denmark, DK-2800 Kgs. Lyngby, Denmark
niet@risoe.dtu.dk

Abstract

The influence of ground proximity and/or wind shear on the power production of a wind turbine is studied using full Navier-Stokes simulations combined with an actuator disc approach. The work reveals that the local power coefficient of a disc operating in a sheared inflow at a given local thrust coefficient is higher than in a corresponding uniform inflow. When a ground surface is present, it is shown that the increased power production, caused by the wind shear, decreases with decreasing hub height. If the incoming wind is uniform, then the ground surface does not affect the power production significantly.

1 Introduction

Wind shear and ground proximity play a significant role on the loads and power production of a wind turbine and therefore need to be modelled properly. However, recent studies have indicated significant deficiencies in state-of-the-art models attempting to include the effect of wind shear and/or ground proximity on wind turbine performance [1, 2, 3]. Madsen et al. [3] concluded that, when simulating wind turbines in shear flow the BEM (Blade Element Momentum) based models should be formulated in a local sense, i.e. the local induction should be defined with respect to the local free-stream velocity, in order to get the best results. Besides studying the overall performance of various rotor model approaches, Madsen et al. [3] also investigated the effect of wind shear and ground proximity on the power production of wind turbines. For this study simulations were carried out on a wind turbine operating at nearly optimal loading in respectively uniform and sheared inflow. They found that, despite the available power in the incoming wind being higher when in shear, the power production of the turbine was lower than in uniform inflow. The reason for this, was that the blades of the wind turbine in shear often operated away from optimal conditions.
However, in a recent study [4], employing both an analytical vortex model, and actuator disc computations combined with full Navier-Stokes simulations, it was shown that the local power coefficient of a disc operating in a sheared inflow, at a given prescribed local thrust coefficient (based on local far upstream velocities), was higher than predicted by classical $1D$ momentum theory. The increased power production was shown to be a consequence of the interaction of the wake with the wind shear, which induces a downward velocity (see section 2), which in effect caused high velocity fluid from higher altitudes to be sucked down to the rotor. The existence of downward velocities upstream of a turbine operating in shear flow was also found in full Navier Stokes computations conducted by Zahle and Sørensen [5]. However, even though their simulations showed an increased power production of the turbine in shear, they found that the power coefficient, based on the available power in the in-

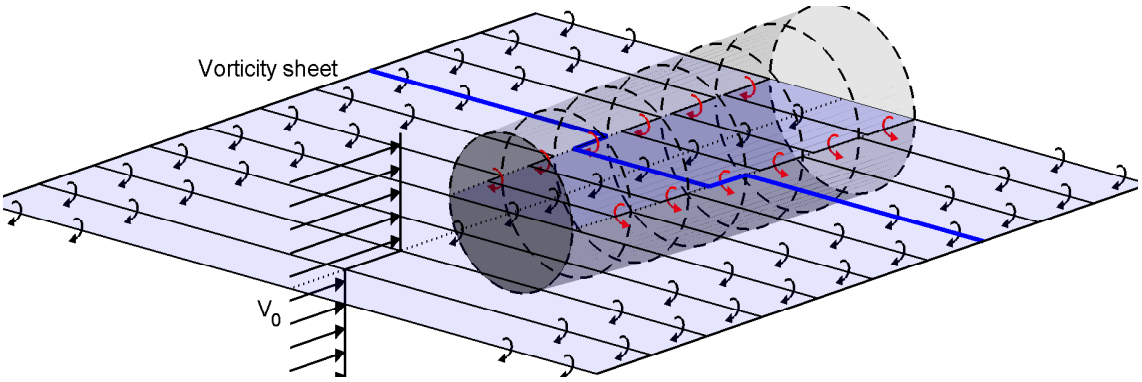

Figure 1: *Sketch of vortex system for a disc operating in a free-stream field with a velocity jump.*

coming wind, was lower than in uniform inflow. Thus, the contribution to the power caused by the generation of a downward induced velocity may be counteracted because the blades often are not operating at optimal conditions.
This paper is a continuation of the actuator disc simulations presented in [4] and focusses on the influence of ground proximity on the power production on the disc.

2 Qualitative considerations

This section presents a qualitative description of the expected effect of wind shear and/or ground proximity on the power production of an axially loaded actuator disc.

2.1 Influence of wind shear

In [4] it was shown that a prescribed loaded actuator disc operating in a wind shear benefits from a higher local power coefficient than a correspondingly loaded disc in a uniform inflow. In order to understand the mechanism responsible for this power increase, consider an axially loaded actuator disc operating in a steady incompressible flow field with a free-stream velocity V_0, which may vary in space.
The axial loading applied on the disc is denoted f ($f = dT/dA$) and a local thrust coefficient is defined as:

$$C_{T,loc}(r,\theta) = \frac{f(r,\theta)}{\frac{1}{2}\rho V_0^2(r,\theta)} \tag{1}$$

where ρ is the air density and f, V_0 and $C_{T,loc}$ may vary in space as indicated.
Similarly, a local induction factor in the rotor plane and a power coefficient are defined as:

$$a_{z,loc}(r,\theta) = \frac{V_0(r,\theta)-V_z(r,\theta)}{V_0(r,\theta)} \tag{2}$$

$$C_{P,loc}(r,\theta) = \frac{f(r,\theta)V_z(r,\theta)}{\frac{1}{2}\rho V_0^3(r,\theta)} \tag{3}$$

where V_z denotes the local axial velocity in the rotor plane.
In order to describe the basic mechanisms, we consider the case where the wind shear is modelled as a jump in the streamwise velocity, where the inflow velocity on the upper half of the disc is $V_\infty + \Delta V/2$ while it on the lower half is $V_\infty - \Delta V/2$, see Figure 1. The discontinuous change in the velocity is obtained by introducing a continuous sheet of vortices with local sheet strength $\gamma = \Delta V$ in the horizontal plane through the center axis of the rotor. This vortex sheet is in the following considered consisting of an infinite number of straight vortex filaments, one of which is highlighted in blue in the figure.
In the wake of the disc the velocity is reduced compared to the ambient flow and therefore

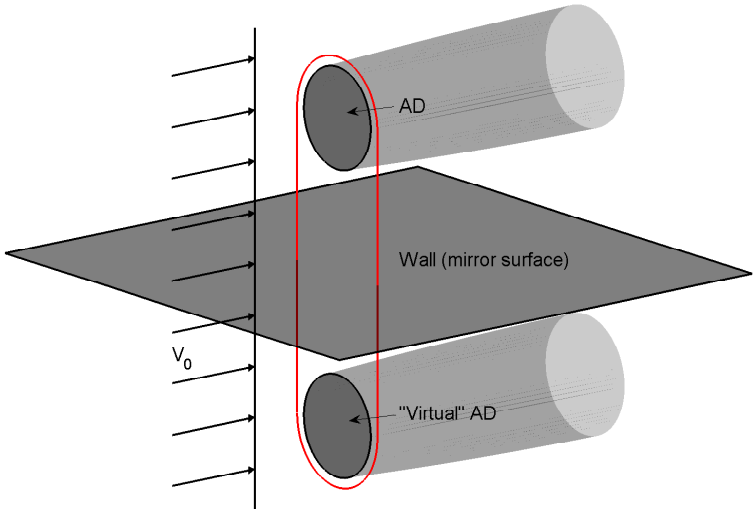

Figure 2: *Sketch of disc operating in a uniform inflow near a ground surface, where the ground is modelled using mirror elements. The red curve illustrates how the two discs, can be regarded as a large non-uniformly loaded actuator disc.*

the part of the vortex filaments, which are inside the wake is convected slower downstream than the parts that are outside. As a consequence, the vortex filaments are stretched at the wake boundary, which in turn (as indicated with red arrows in Figure 1) causes axial vorticity to be formed here. This axial vorticity induces a downwards velocity component and hence the vorticity sheet (that is responsible for the velocity jump) is deflected downwards. In effect this causes a larger part of the disc to be subject to a high velocity and thus the disc will produce more power.

2.2 Influence of ground proximity

The expected effect of ground proximity can best be understood by considering the ground as a mirror surface (see Figures 2-3), which is the way the wall is modelled in the vortex model described in [4]. The introduction of a mirror surface implies that there is a "virtual" disc operating below ground level, with the same distance to the ground as the "real" disc.
If the incoming wind, as sketched in 2, is uniform, then the presence of a ground surface is not expected to affect the power production of the disc. This presumption is based on the work in [4] where it was shown that $C_{P,loc}$ of a non-uniformly loaded actuator disc operating in a uniform inflow corresponds very well to the predictions of $1D$ momentum theory. Since a disc operating in a uniform inflow near a wall (mirror surface), as sketched with a red closed curve in Figure 2, can be seen as a large non-uniformly loaded actuator disc operating in a uniform inflow, it follows from the finding in [4] that $C_{P,loc}$ should be relatively unaltered by the presence of a ground surface if there is no wind shear.
The combined effect of ground proximity and wind shear on the power production of a prescribed loaded actuator disc was touched upon in [4] by means of a simple vortex model. It was found that the presence of a slip-wall reduces the downward induced velocity and hence also the positive effect of the wind shear on the power production, c.f. the description given in the previous section. The reason for this is again best realized by regarding the ground as

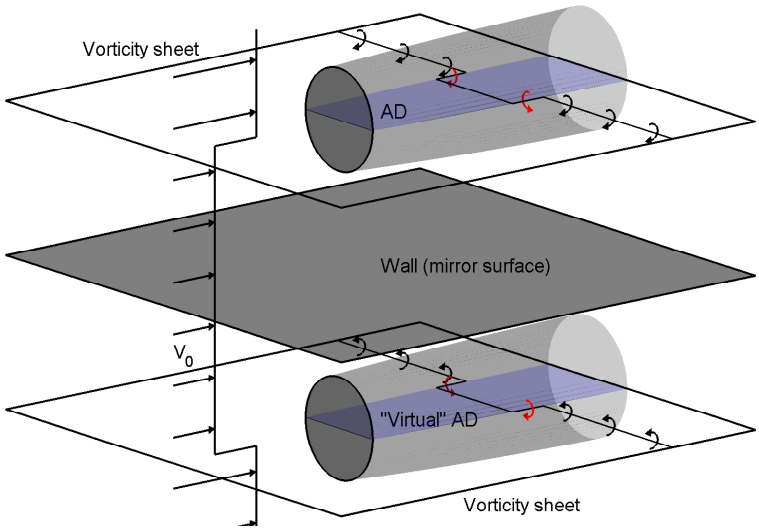

Figure 3: *Sketch of disc operating in wind shear near a ground surface, where the ground is modelled using mirror elements.*

a mirror surface as sketched in Figure 3. Obviously, the "virtual" disc located below ground level, by the same mechanisms as described in the previous section, induces a vertical velocity in the opposite direction to the "real" disc, thereby counter acting the mechanism responsible for the power increase.

3 Numerical methods

This section describes the various models employed for the simulations.

3.1 The generalized actuator disc model

The actuator disc model used in the present work is described in [4, 8] and was originally developed by Mikkelsen as an extension of the model presented in [7]. The model combines the Navier-Stokes flow solver EllipSys3D with an actuator disc technique where body forces are distributed on a disc representing a wind turbine rotor. Hence, the basis of the method is the incompressible Navier-Stokes equations

$$\begin{aligned} \frac{\partial \boldsymbol{V}}{\partial t} + \boldsymbol{V} \cdot \nabla \boldsymbol{V} &= -\tfrac{1}{\rho}\nabla p + \nu \nabla^2 \boldsymbol{V} + \boldsymbol{f'} \\ \nabla \cdot \boldsymbol{V} &= 0 \end{aligned} \tag{4}$$

where $\boldsymbol{f'}$ denote the body forces, which represent the loading on the disc.
As sketched in Figure 4, a local polar grid is used to represent the loading on the disc, while the surrounding flowfield is solved in a Cartesian mesh. The loading applied to each differential area of the disc is denoted $\boldsymbol{f}$ and the corresponding volume force is $\boldsymbol{f'} = f/dz$, where dz is the length of a computational cell in the flow direction.
The applied disc forces needs to be distributed smoothly on several mesh point to avoid singular behavior. In practice, the smearing is carried out in two steps by distributing the forces in the directions respectively radially and perpendicularly to the disc in a $1D$ Gaussian manner. Initially, the loading is smeared in the radial direction by taking the convolution of the computed load $\boldsymbol{f'}$, and a regularization kernel η_{ϵ_r}:

$$\begin{aligned} \boldsymbol{f'}_{\epsilon_r} &= \boldsymbol{f'} \otimes \eta_{\epsilon_r} \\ \eta_{\epsilon_r}(r) &= \frac{\exp\left[-\left(\frac{r}{\epsilon_r}\right)^2\right]}{\epsilon_r \sqrt{\pi}} \end{aligned} \tag{5}$$

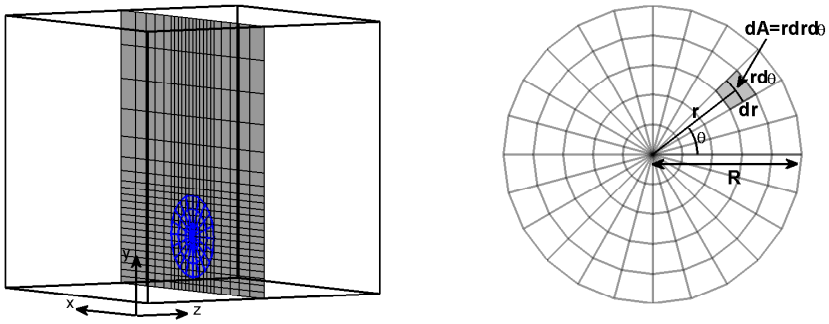

Figure 4: *Sketch of computational domain and actuator disc*

where ϵ_r is a parameter that serves to adjust the concentration of the regularized load. Inserting gives the distributed force

$$\boldsymbol{f'}_{\epsilon_r}(r,\theta) = \int_{-\infty}^{\infty} \frac{\boldsymbol{f'}(r',\theta)}{\epsilon_r\sqrt{\pi}} \exp\left[-\left(\frac{r-r'}{\epsilon_r}\right)^2\right] \mathrm{d}r' \tag{6}$$

The final regularized force is subsequently obtained by smearing the loading $\boldsymbol{f'}_{\epsilon_r}$ in the direction normal to the disc using a similar approach:

$$\boldsymbol{f'}_{\epsilon_{nr}}(r,\theta,z) = \int_{-\infty}^{\infty} \frac{\boldsymbol{f'}_{\epsilon_r}(r,\theta)}{\epsilon_n\sqrt{\pi}} \exp\left[-\left(\frac{d}{\epsilon_n}\right)^2\right] \mathrm{d}n \tag{7}$$

where d is the distance between cell centered grid points and the rotor disc and ϵ_n is a smearing parameter.
In all simulations of the present work the smearing parameters are $\epsilon_z = \epsilon_r = 3dr$, where dr is the grid spacing. This choice is based on the suggestions provided in [4].

3.2 Flow solver - EllipSys3D

The flow field was computed using the EllipSys3D incompressible Navier Stokes flow solver developed by Michelsen [9], [10] and Sørensen [11]. This code solves the discretized Navier-Stokes equations in general curvilinear coordinates using a block structured finite volume approach. The solver is formulated in primitive variables (pressure-velocity) in a collocated grid arrangement. The pressure correction equation was solved using the SIMPLE algorithm, and pressure decoupling is avoided using Rhie/Chow interpolation and the convective terms were discretized using the third order accurate QUICK scheme.
All simulations in the present work are carried out at a Reynolds number of, $Re = RV_\infty/\nu = 10^4$, which was shown in [4] to be sufficiently high to get Reynolds number independent solutions.

3.3 Modelling the wind shear

The wind shear profile is imposed by introducing body forces to the entire computational domain. The used technique was originally presented by Mikkelsen et al. [13] and is described in more detail in [6]. The idea is to conduct an initial computation without the wind turbine included in the domain in order to establish the force field required to obtain a desired mean wind shear profile. The obtained steady force field is afterward stored and fixed in the computation where the wind turbine is included.

3.4 Computational domain & boundary conditions

A schematic of the mesh layout is shown in Figure 4. The computational domain is cubic with a side length of 24 rotor radii. In all simulation, the disc center is positioned at hub height ($y = H$) in the center of the domain and directed perpendicular to the flow direction (z-direction). A high concentration of grid points is distributed equidistantly in the vicinity of the rotor in order to resolve the strong gradients here. The grid consisted of 128 grid points in each direction, and in the equidistant region a rotor radius was resolved with 30 grid points, i.e. $dr = R/30$. The boundary conditions were as follows: The velocity was specified according to the wanted profile at the inlet (Dirichlet condition), zero velocity gradient at the outlet (Neumann condition), periodic conditions on the sides, symmetry at the top boundary and no-slip or symmetry at the bottom boundary.

4 Results

In the following the results of the simulations of the influence of ground proximity and/or shear on the power production of the disc is presented. The following cases are considered:

- A disc with constant $C_{T,loc}$ in a non-sheared inflow at various heights above a slip wall.
- A disc with constant $C_{T,loc}$ in a sheared inflow at various heights above a slip wall.
- A disc with constant $C_{T,loc}$ in a sheared inflow at various heights above a no-slip wall.

In all cases, the results are compared with the corresponding predictions on a constant loaded actuator disc operating in a uniform inflow.

4.1 Proximity to a slip wall - uniform inflow

A disc with constant $C_{T,loc} = C_{T,0}$, operating in uniform inflow ($V_0(r,\theta) = V_\infty$) at various heights above a slip wall is considered.

Figure 5 displays the circumferentially averaged axial induction factor in the rotor plane for two different hub heights for a disc with $C_{T,0} = 0.89$. As seen the curves nearly collapse on single curve, which is consistent with the considerations made in section 2. The small difference may be due to confinement of the flow below the rotor. To obtain a more clear picture of the influence of ground proximity in a non-sheared inflow, Figures 6-7 show the integrated quantities a_z and C_P as a function of hub height at different thrust coefficients. In order to exclude the part of the disc that is affected by the radial smearing of the disc forces (see section 3.1) the integrated quantities are here defined as:

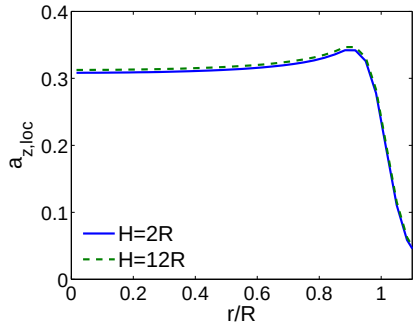

Figure 5: *Circumferentially averaged $a_{z,loc}$ in the rotor plane for a disc with $C_{T,0} = 0.89$ in uniform inflow at two different hub heights.*

$$\begin{aligned} a_z &= \frac{\int_0^{2\pi}\int_0^{R-3dr} a_{z,loc} r dr d\theta}{\pi(R-3dr)^2} \\ C_P &= \frac{\int_0^{2\pi}\int_0^{R-3dr} C_{P,loc} r dr d\theta}{\pi(R-3dr)^2} \end{aligned} \quad (8)$$

Note that for convenience, both quantities are scaled with their respective values obtained at hub height $H = 12R$ in the plots. As seen there is a trend of reduced induction (and thus increased power) with decreasing hub height,

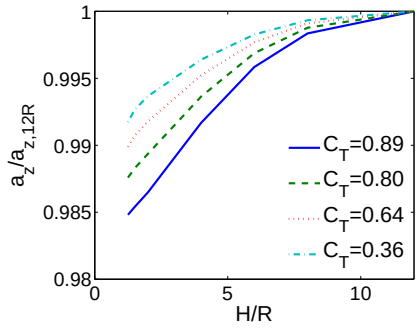

Figure 6: *Variation of a_z as a function of hub height for different C_T levels, plotted as a fraction of a_z for a corresponding disc with $H = 12R$. The incoming wind is uniform and the ground is modelled as a slip wall.*

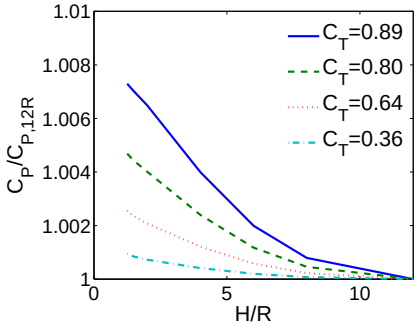

Figure 7: *C_P as a function of hub height for different C_T levels, plotted as a fraction of C_P of a corresponding disc with $H = 12R$. The incoming wind is uniform and the ground is modelled as a slip wall.*

which becomes increasingly pronounced with increasing C_T. However, the difference in power production near and far away from the ground is in all cases less than one percent, which suggests that the assumption made in the simple vortex model is valid (see section 2).

4.2 Proximity to a slip wall - sheared inflow

In the following a disc with constant $C_{T,loc} = C_{T,0}$ operating in a sheared inflow near a slip wall is considered. Note that a constant $C_{T,loc}$ does not imply a constant thrust on the disc in this case because the free-stream velocity is varying in space. The velocity profile is modelled in the following way:

$$\frac{V_0(y)}{V_\infty} = \begin{cases} 1 - 3\alpha & \text{if } \frac{y-H}{R} < -3, \\ 1 + \alpha\frac{y-H}{R} & \text{if } -3 \leq \frac{y-H}{R} \leq 3, \\ 1 + 3\alpha & \text{if } \frac{y-H}{R} > 3. \end{cases} \quad (9)$$

where V_∞ is the undisturbed wind speed at hub height, R is the rotor radius, y is the vertical coordinate, which is zero at the ground, H is the hub height and $\alpha = 0.25$ is a constant.

Figures 8-9 display a_z and C_P (see equation 8) as a function of hub height for different thrust coefficients. As in Figures 6-7, both quantities are scaled with the corresponding result obtained in uniform inflow at hub height $H = 12R$. In this way, the figures directly show the influence of shear and ground proximity on the induction and power coefficient of the disc. As seen the induction clearly increases (and thus the power coefficient decreases) with decreasing hub height, which is in good agreement with the explanation presented in section 2 and illustrated in Figure 3. Furthermore, it is observed that the described trend becomes increasingly apparent with increasing thrust coefficient. It is further noted that the presence of the ground, in all cases, has almost no effect on the induction and power coefficient for hub heights greater than $4R$. Finally, it should be noted that $C_{P,loc}$, for all hub heights, is higher than in a corresponding uniform inflow. This contradicts the findings of Madsen et al. [3] and Zahle and Sørensen [5] as mentioned in section 1. The reason for this, is that the loading on the actuator disc in the present work is constant and hence is not coupled to the local flow field through the rotor.

In order to give a more clear impression of the influence of shear and wall proximity on the actual power production, the integrated power

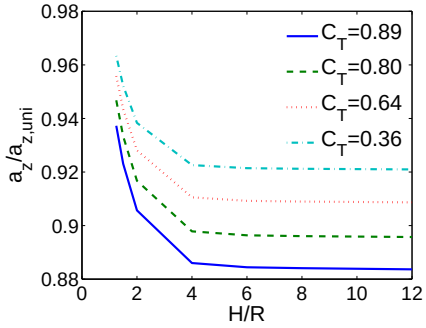

Figure 8: *Variation of a_z as a function of hub height for different C_T levels, plotted as a fraction of a_z of a corresponding disc in uniform inflow with $H = 12R$. The incoming wind is sheared and the ground is modelled as a slip wall.*

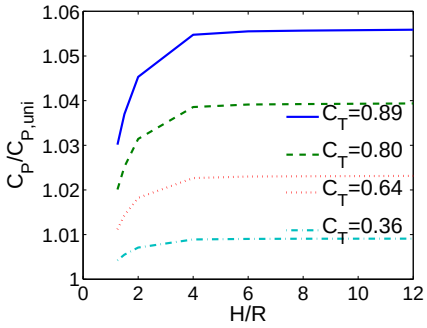

Figure 9: *C_P as a function of hub height at different C_T levels, plotted as a fraction of C_P of a corresponding disc in uniform inflow with $H = 12R$. The incoming wind is sheared and the ground is modelled as a slip wall.*

flux through the disc was computed as:

$$P = \frac{1}{2}\rho \int_A V_0(r,\theta)^3 C_{p,loc}(r,\theta) dA \qquad (10)$$

Figure 10 shows the integrated power flux through the disc as a function of hub height. For convenience the power flux is plotted as a fraction of the power flux obtained in uniform inflow at hub height $H = 12R$. Thereby, the figure shows how much more power is produced in case of shear than in uniform inflow. As seen the trend is the same as in Figure 9, however, the gain of the shear on the power production is less than on $C_{P,loc}$. The reason for this is, as shown in [4], that $C_{P,loc}$ generally is highest on the lower part of the disc where the free-stream velocity is low.

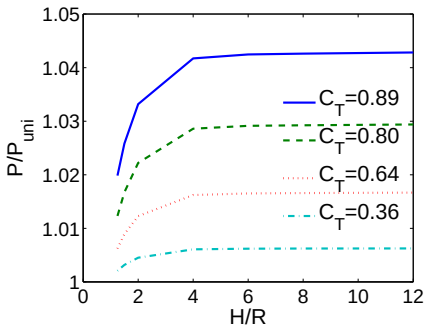

Figure 10: *P as a function of hub height, at different C_T levels, plotted as a fraction of P through a corresponding disc in uniform inflow with $H = 12R$. The incoming wind is sheared and the ground is modelled as a slip wall.*

4.3 Proximity to a no-slip wall - sheared inflow

In this section the results of the simulations on a disc with constant $C_{T,loc} = C_{T,0}$ operating in a sheared inflow near a no-slip wall is considered. The objective of the study is primarily to verify that the conclusions drawn in the previous section with a slip wall are not affected by a more realistic modelling of the ground. The incoming velocity profile is modelled in the following way:

$$\frac{V_0(y)}{V_\infty} = \begin{cases} y\,(c_2 y + c_1) & \text{if } \frac{y}{R} < \frac{\Delta}{R}, \\ 1 + \alpha\frac{y-H}{R} & \text{if } \frac{\Delta}{R} \le \frac{y}{R} \le \frac{H}{R} + 3, \\ 1 + 3\alpha & \text{if } \frac{y}{R} > \frac{H}{R} + 3. \end{cases} \qquad (11)$$

where

$$\begin{aligned} c_2 &= \tfrac{H\alpha - R}{R\Delta^2} \\ c_1 &= \tfrac{1}{R}\left(\alpha - 2\tfrac{H\alpha - R}{\Delta}\right). \end{aligned} \qquad (12)$$

The given values of c_1 and c_2 ensure a smooth transition from the parabolic profile near the wall to the linear profile near the rotor.

Figure 11 compares the variation of C_P (equation 8) as a function of hub height, predicted using respectively a slip wall and a no-slip wall. Once again, C_P is scaled with the corresponding result obtained in uniform inflow at hub height $H = 12R$. From the figure it is evident that, using a no-slip wall instead of a slip wall, only affects the results marginally and thus, the conclusions drawn in the previous section are also valid when using a no-slip wall.

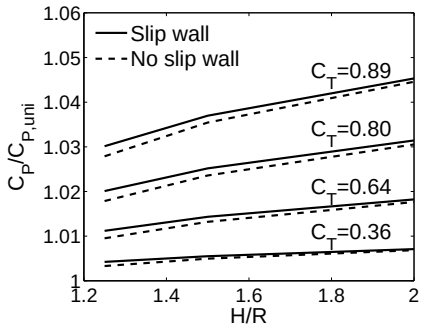

Figure 11: *C_P as a function of hub height in a sheared inflow at different C_T levels using respectively a slip wall and a no-slip wall. C_P is plotted as a fraction of C_P of a corresponding disc in uniform inflow with $H = 12R$.*

5 Conclusion

The influence of ground proximity and/or wind shear on the power production of a wind turbine has been analyzed using an actuator disc technique combined with solution of the Navier-Stokes equations.

The local power coefficient of the disc, at a given thrust coefficient, was shown to be quite insensitive to the presence of a slip wall if the incoming wind is uniform.

For a disc operating in the proximity of a slip wall in a sheared inflow, it was, on the other hand, found that the power production generally decreased with decreasing hub height. However, for all hub heights the local power coefficient, at a given local thrust coefficient (using local free-stream velocities as reference), was higher than in a corresponding uniform inflow.

Finally, it was shown that, using a no-slip wall instead of a slip wall to represent the ground surface does not affect the predicted power production of the disc significantly.

References

[1] Madsen H. Aa. et al. Short-comings in state of the art engineering aerodynamic and aeroelastic models by comparison to advanced models. UPWIND report deliverable 2.2, May 7, 2008.

[2] Madsen et al. Influence of wind shear on rotor aerodynamics, power and loads. In: Research in aeroelasticity EFP-2006. Risø-R-1611(EN) (2007) edited by C.Bak. pp 101-116.

[3] 4. Madsen, H.Aa. et al. BEM modeling of inflow with shear in comparison with CFD validation results 2001. Torque conference, 2010.

[4] Troldborg, N., Gaunaa, M. and Mikkelsen, R. Actuator Disc Simulations of Influence of Wind Shear on Power Production of Wind Turbines. Torque conference, 2010.

[5] Zahle, F. and Sørensen N.N. Navier-Stokes Rotor Flow Simulations with Dynamic Inflow. Torque Conference, Crete, Greece, 2010.

[6] Actuator Line Modeling of Wind Turbine Wakes. PhD thesis, Technical University of Denmark, 2008.

[7] Mikkelsen, R., Actuator Disc Methods Applied to Wind Turbines, MEK-FM-PHD 2003-02, Technical University of Denmark, 2003.

[8] Ivanell, S.S.A. Numerical Computations of Wind Turbine Wakes, PhD Thesis, Linné Flow Centre, KTH Mechanics, Stockholm, Sweden, 2009.

[9] Michelsen, J.A. Basis3D - a Platform for Development of Multiblock PDE Solvers. Report AFM 92-05, Dept. of Fluid Mechanics, Technical University of Denmark, DTU, 1994.

[10] Michelsen, J.A., Block Structured Multigrid Solution of 2D and 3D elliptic PDE's, Report AFM 94-06, Dept. of Fluid Mechanics, Technical University of Denmark, DTU, 1994.

[11] Sørensen, N.N., General Purpose Flow Solver Applied to Flow over Hills, PhD Dissertation, Risø-R-827(EN), RisøNational Laboratory, Roskilde, Denmark, 1995.

[12] Mikkelsen, R., Sørensen, J.N. and Shen, W.Z. Modelling and Analysis of the Flow Field around a Coned Rotor. Wind Energy, 4: 121-135, 2001.

[13] Mikkelsen, R., Sørensen, J.N. and Troldborg, N. Analysis of Power Enhancement for a Row of Wind Turbines Using the Actuator Line Technique. TWIND. Technical University of Denmark, Lyngby, August 2007.